



3 1176 00084 3012

CONFIDENTIAL

Copy 5
RM L53K09

NACA RM L53K09



RESEARCH MEMORANDUM

FOR INTERNAL USE ONLY

NOT TO BE RELEASED FROM THIS OFFICE

MEASURED AND ESTIMATED LATERAL STATIC AND ROTARY

DERIVATIVES OF A 1/12-SCALE MODEL OF A

HIGH-SPEED FIGHTER AIRPLANE

WITH UNSWEPT WINGS

By James L. Williams

Langley Aeronautical Laboratory
Langley Field, Va.

LIBRARY COPY

JAN 19 1954

LANGLEY AERONAUTICAL LABORATORY
LIBRARY, NACA
LANGLEY FIELD, VIRGINIA

CLASSIFIED DOCUMENT

This material contains information affecting the National Defense of the United States within the meaning of the espionage laws, Title 18, U.S.C., Secs. 793 and 794, the transmission or revelation of which in any manner to an unauthorized person is prohibited by law.

NATIONAL ADVISORY COMMITTEE FOR AERONAUTICS

WASHINGTON

January 11, 1954

CLASSIFICATION CANCELLED

Authority: *NACA Rep. Res. - 11-11-56*
x *RN-109*
By: *DA 11-30-56* SOG

CONFIDENTIAL

NATIONAL ADVISORY COMMITTEE FOR AERONAUTICS

RESEARCH MEMORANDUM

MEASURED AND ESTIMATED LATERAL STATIC AND ROTARY

DERIVATIVES OF A 1/12-SCALE MODEL OF A

HIGH-SPEED FIGHTER AIRPLANE

WITH UNSWEPT WINGS

By James L. Williams

SUMMARY

A low-speed investigation was made in the Langley stability tunnel in order to determine the lateral static and rotary derivatives of a 1/12-scale model of a high-speed fighter airplane. The experimental results obtained through the complete angle-of-attack range are presented primarily for reference purposes. However, a detailed comparison at three angles of attack of the lateral static and rotary derivatives estimated by currently available methods with the experimental lateral static and rotary derivatives is made. In general, the vertical-tail contributions to the static and rotary derivatives could be estimated with a good degree of accuracy. The estimated wing-fuselage-combination derivatives, however, were not in good agreement with the measured values. The lack of better agreement of the estimated and measured derivatives of the wing-fuselage combination may be caused by the interference of the thick wing roots at the wing-fuselage juncture which could not be accounted for by the methods employed and the inability to calculate readily the fuselage-alone contribution to certain of the stability derivatives.

INTRODUCTION

Several methods are available for estimating stability derivatives of airplanes (for example, see ref. 1); however, these methods do not account well for the effect of unusual airplane geometry on the stability derivatives. This deficiency often results in a poor prediction of the dynamic stability characteristics of the airplane. A similar situation appears to exist for the high-speed fighter airplane employed in this investigation since the damping of the lateral

oscillation of this airplane could not be calculated in one investigation with the accuracy desired by using estimated stability derivatives (ref. 2) although better agreement was obtained in another investigation (ref. 3).

The purpose of the present investigation, which was made in the Langley stability tunnel, was to obtain the low-speed lateral static and rotary stability derivatives of a 1/12-scale model of a high-speed fighter airplane with unswept wings and to compare the experimental stability derivatives with the derivatives estimated by current methods for the wing-fuselage combination, the vertical- and horizontal-tail combination, and the complete model. In addition, since a large difference existed between the static lateral stability derivatives presented herein and the unpublished derivatives obtained in previous tests of a sting-supported model, a few tests were made to determine the effects on the static lateral stability derivatives of a fuselage modification similar to that necessitated for sting-mounting. This modification consisted of an increase in the cross-sectional area of the rear portion of the fuselage under the vertical tail.

SYMBOLS AND COEFFICIENTS

The data presented herein are in the form of standard NACA coefficients of forces and moments which are referred to the stability system of axes (fig. 1) with the origin at the projection of the 0.23 point of the wing mean aerodynamic chord on the plane of symmetry. The positive directions of the forces, moments, and angular displacements are shown in figure 1. The symbols and coefficients are defined as follows:

- b span, ft
- c wing chord, parallel to plane of symmetry, ft
- \bar{c} mean aerodynamic chord, $\frac{2}{S} \int_0^{b/2} c^2 dy$, ft
- y spanwise distance measured from and perpendicular to plane of symmetry, ft
- p rolling angular velocity, radians/sec
- r yawing angular velocity, radians/sec
- q dynamic pressure, $\frac{1}{2}\rho V^2$, lb/sq ft

S	area, sq ft
V	free-stream velocity, ft/sec
α	angle of attack of fuselage reference line (parallel to wing line 0), deg
β	angle of sideslip, deg
ψ	angle of yaw, deg
ρ	mass density of air, slugs/cu ft
L	lift, lb
D	drag, lb
Y	lateral force, lb
M	pitching moment, ft-lb
N	yawing moment, ft-lb
L'	rolling moment, ft-lb
C_L	lift coefficient, L/qS_W
C_D	drag coefficient, D/qS_W
C_Y	lateral-force coefficient, Y/qS_W
C_m	pitching-moment coefficient, $M/qS_W\bar{c}_W$
C_n	yawing-moment coefficient, N/qS_Wb_W
C_l	rolling-moment coefficient, L'/qS_Wb_W

$$C_{L\alpha} = \frac{\partial C_L}{\partial \alpha}$$

$$C_{Y\beta} = \frac{\partial C_Y}{\partial \beta}$$

$$C_{n\beta} = \frac{\partial C_n}{\partial \beta}$$

$$C_{l_\beta} = \frac{\partial C_l}{\partial \beta}$$

$$C_{Y_p} = \frac{\partial C_Y}{\partial \frac{pb}{2V}}$$

$$C_{n_p} = \frac{\partial C_n}{\partial \frac{pb}{2V}}$$

$$C_{l_r} = \frac{\partial C_l}{\partial \frac{rb}{2V}}$$

$$C_{Y_r} = \frac{\partial C_Y}{\partial \frac{rb}{2V}}$$

$$C_{n_r} = \frac{\partial C_n}{\partial \frac{rb}{2V}}$$

$$C_{l_r} = \frac{\partial C_l}{\partial \frac{rb}{2V}}$$

Subscripts:

- W wing
 H horizontal tail
 V vertical tail

Model components:

- WF wing and fuselage
 VH vertical and horizontal tails
 WFVH wing, fuselage, and vertical and horizontal tails
 (complete model)

APPARATUS, MODEL, AND TESTS

The tests of the present investigation were made in the 6-foot-diameter rolling-flow test section (ref. 4) and the 6- by 6-foot curved-flow test section (ref. 5) of the Langley stability tunnel in which rolling or yawing flight is simulated by rolling or curving the air-stream about a stationary model.

The model was mounted on a rigid single-strut support at the projection of the 0.23 point of the mean aerodynamic chord of the wing on the plane of symmetry. The 1/12-scale fighter airplane model used in the present tests was constructed of laminated mahogany with aluminum inserts along the trailing edge of the wing. The model was designed to permit tests of the wing-fuselage combination alone or with vertical and horizontal tails. There was no air flow through the simulated jet ducts in the wing roots. A sketch of the complete model is presented in figure 2 and photographs of the model are presented as figure 3. A list of pertinent geometric characteristics is given in table I.

The forces and moments were measured by means of a six-component-balance system through an angle-of-attack range of about -4° to 20° . The test conditions are summarized in the following table:

Test	β , deg	$\frac{pb}{2V}$	$\frac{rb}{2V}$	Mach number	Reynolds number
Static longitudinal	0	-	-	0.17	0.73×10^6
Static lateral	$\pm 6, \pm 4, \pm 2, 0$	-	-	.17	.73
Rolling	0	0 ± 0.0172 ± 0.0342 ± 0.0520	-	.17	.73
Yawing	0	-	0 -.0359 -.0761 -.1002	.13	.57

The wing-fuselage combination and the complete model were tested for each of the conditions listed in the preceding table. Tests were also made at $\alpha = 0^\circ$ and $\beta = \pm 5^\circ$ and 0° with the wing-fuselage

combination and complete model with the rear portion of the fuselage under the vertical tail modified (fig. 4) to simulate the sting-supported model employed in previous tests of this model.

CORRECTIONS

Approximate jet-boundary corrections as determined by the methods of reference 6 were applied to the angles of attack and drag coefficients. Horizontal-tail-on pitching moments were corrected for the effects of jet boundary by the methods of reference 7. However, the data have not been corrected for blockage effects which were considered negligible.

The lateral-force coefficients have been corrected for the buoyancy effect due to the static-pressure gradient across the curved-flow test section (ref. 5), but the data have not been corrected for support-strut tares which, with the exception of the drag tare, are believed to be small. The absolute values of the drag coefficients therefore should not be representative of the free-air values.

RESULTS AND DISCUSSION

Presentation of Data

The figures in which the data obtained from wind-tunnel tests made to determine the low-speed lateral static and rotary derivatives of a 1/12-scale model of a high-speed fighter airplane with unswept wings are summarized in the following table:

Data	Figure
C_m , C_L , and C_D plotted against α	5
C_{Y_β} , C_{n_β} , and C_{l_β} plotted against α	6
C_{Y_p} , C_{n_p} , and C_{l_p} plotted against α	7
C_{Y_r} , C_{n_r} , and C_{l_r} plotted against α	8

The experimentally determined derivatives for the 1/12-scale fighter airplane model through the complete angle-of-attack range are presented primarily for reference purposes; however, a detailed comparison at three angles of attack of the lateral static and rotary derivatives estimated by currently available methods with the experimental lateral static and rotary derivatives is presented in figure 9.

Effect of Fuselage Modification on Static Lateral Derivatives

A comparison of the static lateral stability derivatives obtained in the present investigation (fig. 6) with some unpublished results obtained at a Mach number of 0.4 indicates larger differences than would be expected to be caused by Mach number effects alone. The model employed in the tests at a Mach number of 0.4 was sting supported with the sting entering the rear portion of the fuselage. This arrangement necessitated a revision to the fuselage aftersection because of the fuselage shape (see fig. 2). In order to determine the importance of this modification on the static lateral characteristics, the fuselage of the model used in the stability-tunnel investigation was modified (see fig. 4) to simulate this sting-supported model. The derivatives resulting from tests of this arrangement are presented in figure 6. The values of the modified-fuselage derivatives are in good agreement with the unpublished derivatives obtained at a Mach number of 0.4. The fuselage modification produced a large increase in $C_{Y\beta_V}$ and $C_{n\beta_V}$ (see fig. 6). These changes are believed to result from the increase in end-plate effect and the induced sidewash of the fuselage on the vertical tail as the fuselage size under the tail is increased. The use of values of $C_{Y\beta_V}$ from the sting-supported-model tests in estimating $C_{n_{rV}}$ would give erroneous results, of course.

It appears, therefore, that in testing models similar to the model of the present investigation an effort should be made to minimize fuselage modifications. If the effect of fuselage modification on the test results cannot be evaluated by experimental or theoretical methods, then it may be necessary to mount the model on wing-tip stings which would require, of course, the determination of tares.

Estimation of Derivatives and Comparison With Experiment

Wing-fuselage contribution.- The procedure employed for estimating the wing-fuselage combination derivatives except as noted for C_{n_r} and C_{n_p} was to estimate the wing and fuselage derivatives separately and to add them algebraically. The derivatives of the basic wing plan form and fuselage were obtained from the following sources:

Component	Derivative	Reference
Wing	C_{l_β} , C_{n_β} , C_{Y_β} , C_{l_r} , C_{n_r} , and C_{Y_r}	8
Wing	C_{l_p}	9
Wing	C_{Y_p} and C_{n_p}	10
Fuselage	C_{Y_β} and C_{n_β}	11
Fuselage	C_{Y_r}	12
Fuselage	C_{Y_p}	13
Fuselage	C_{l_β} , C_{l_r} , and C_{l_p}	Assumed to be zero

The lift and drag data of the wing-fuselage combination (fig. 5) were used with the methods of references 8 and 10 to estimate C_{n_r} and C_{n_p} and no additional increments were added for the fuselage since it is indirectly accounted for in this manner. The effect of wing dihedral on C_{Y_p} was determined from reference 14 and on C_{l_β} and C_{l_r} from references 15 and 16, respectively. The effect of wing position on the sideslip derivatives was determined from reference 17 assuming a low-wing position. The mutual-interference effects of the wing-fuselage combination have not been accounted for in these calculations since all the currently available interference data have been determined for simple bodies of revolution only (refs. 11, 12, and 18). There was no air flow through the wing ducts. It is believed that for this case the flow through the ducts has no appreciable effect on the stability derivatives.

In general the estimated derivatives of the wing-fuselage combination are only in fair agreement with the measured derivatives (see fig. 9). It appears that this lack of better agreement could be caused by a large interference effect of the thick wing roots at the wing-fuselage juncture which cannot be accounted for by the currently available methods, and the inability to calculate readily an accurate fuselage-alone contribution to some of the stability derivatives. Evidently, more information on the mutual-interference effects for wing-fuselage combinations other than simple bodies of revolution is needed.

Vertical-tail contribution.- The vertical-tail increments to the stability derivatives were calculated by means of the equations given

in reference 19. The lift-curve slope $C_{L_{\alpha y}}$ was determined from reference 20 for an effective aspect ratio determined from references 11 and 17. In the estimation of the yawing and rolling derivatives of the vertical tail the effective aspect ratio was considered to be equal to the geometric aspect ratio with no end-plate effect of the fuselage.

A comparison of the estimated and measured tail contribution to the various derivatives is presented for three angles of attack in figure 9. The estimated increments in the lateral static and rotary derivatives due to the tail are generally in good agreement with the measured values. An exception is noted for the vertical-tail contribution to the rolling derivatives where, although the trend with angle of attack is estimated accurately, the magnitude of these increments is in some cases of opposite sign to the experimental increments. It is believed that the thick wing roots at the wing-fuselage juncture produced sidewash at the vertical tail that cannot be accounted for by the methods employed in this paper. Because of its location the horizontal tail was felt to have little influence on the vertical tail; hence this effect was not accounted for in this paper.

Complete model.- The estimated derivatives for the wing-fuselage combination and tail group were summed to obtain the complete model derivatives. The agreement between the estimated and measured derivatives was generally good. The poor agreement between certain estimated and measured complete-model derivatives is obtained as a direct consequence of the inability to estimate the wing-fuselage contribution to the derivatives.

CONCLUDING REMARKS

A low-speed investigation was made in the Langley stability tunnel in order to determine the lateral static and rotary derivatives of a 1/12-scale model of a high-speed fighter airplane with unswept wings. The experimentally determined derivatives through the complete angle-of-attack range are presented primarily for reference purposes. However, a detailed comparison at three angles of attack of the lateral static and rotary derivatives estimated by currently available methods with the experimental derivatives is presented.

In using current methods to estimate the derivatives of the airplane it was found that in general the tail contribution to the lateral static and rotary derivatives could be estimated with a good degree of accuracy. The estimated wing-fuselage-combination derivatives, however, were not in good agreement with the measured values. This lack of better agreement may be caused by the interference of the thick wing roots at the

wing-fuselage juncture which could not be accounted for by the methods employed, and the inability to calculate readily the fuselage-alone contribution to certain of the stability derivatives.

Langley Aeronautical Laboratory,
National Advisory Committee for Aeronautics,
Langley Field, Va., October 26, 1953.

REFERENCES

1. Campbell, John P., and McKinney, Marion O.: Summary of Methods for Calculating Dynamic Lateral Stability and Response and for Estimating Lateral Stability Derivatives. NACA Rep. 1098, 1952. (Supersedes NACA TN 2409.)
2. Crane, H. L., Beckhardt, A. R., and Matheny, C. E.: Flight Measurements of the Lateral Stability and Control Characteristics of a High-Speed Fighter Airplane. NACA RM L52B14, 1952.
3. Heinle, Donovan R., and McNeill, Walter E.: Correlation of Predicted and Experimental Lateral Oscillation Characteristics for Several Airplanes. NACA RM A52J06, 1952.
4. MacLachlan, Robert, and Letko, William: Correlation of Two Experimental Methods of Determining the Rolling Characteristics of Unswept Wings. NACA TN 1309, 1947.
5. Bird, John D., Jaquet, Byron M., and Cowan, John W.: Effect of Fuselage and Tail Surfaces on Low-Speed Yawing Characteristics of a Swept-Wing Model As Determined in Curved-Flow Test Section of the Langley Stability Tunnel. NACA TN 2483, 1951. (Supersedes NACA RM L8G13.)
6. Silverstein, Abe, and White, James A.: Wind-Tunnel Interference With Particular Reference to Off-Center Positions of the Wing and to the Downwash at the Tail. NACA Rep. 547, 1936.
7. Gillis, Clarence L., Polhamus, Edward C., and Gray, Joseph L., Jr.: Charts for Determining Jet-Boundary Corrections for Complete Models in the 7- by 10-Foot Closed Rectangular Wind Tunnels. NACA WR L-123, 1945. (Formerly NACA ARR L5G31.)
8. Toll, Thomas A., and Queijo, M. J.: Approximate Relations and Charts for Low-Speed Stability Derivatives of Swept Wings. NACA TN 1581, 1948.
9. Goodman, Alex, and Adair, Glenn H.: Estimation of the Damping in Roll of Wings Through the Normal Flight Range of Lift Coefficient. NACA TN 1924, 1949.
10. Goodman, Alex, and Fisher, Lewis R.: Investigation at Low Speeds of the Effect of Aspect Ratio and Sweep on the Rolling Stability Derivatives of Untapered Wings. NACA Rep. 968, 1950. (Supersedes NACA TN 1835.)

11. Queijo, M. J., and Wolhart, Walter D.: Experimental Investigation of the Effect of Vertical-Tail Size and Length and of Fuselage Shape and Length on the Static Lateral Stability Characteristics of a Model With 45° Sweptback Wing and Tail Surfaces. NACA Rep. 1049, 1951. (Supersedes NACA TN 2168.)
12. Letko, William: Effect of Vertical-Tail Area and Length on the Yawing Stability Characteristics of a Model Having a 45° Sweptback Wing. NACA TN 2358, 1951.
13. Letko, William, and Riley, Donald R.: Effect of an Unswept Wing on the Contribution of Unswept-Tail Configurations to the Low-Speed Static- and Rolling-Stability Derivatives of a Midwing Airplane Model. NACA TN 2175, 1950.
14. Queijo, M. J., and Jaquet, Byron M.: Calculated Effects of Geometric Dihedral on the Low-Speed Rolling Derivatives of Swept Wings. NACA TN 1732, 1948.
15. Bird, John D.: Some Theoretical Low-Speed Span Loading Characteristics of Swept Wings in Roll and Sideslip. NACA Rep. 969, 1950. (Supersedes NACA TN 1839.)
16. Queijo, M. J., and Jaquet, Byron M.: Investigation of Effects of Geometric Dihedral on Low-Speed Static Stability and Yawing Characteristics of an Untapered 45° Sweptback-Wing Model of Aspect Ratio 2.61. NACA TN 1668, 1948.
17. Goodman, Alex: Effects of Wing Position and Horizontal-Tail Position on the Static Stability Characteristics of Models With Unswept and 45° Sweptback Surfaces With Some Reference to Mutual Interference. NACA TN 2504, 1951.
18. Wolhart, Walter D.: Influence of Wing and Fuselage on the Vertical-Tail Contribution to the Low-Speed Rolling Derivatives of Midwing Airplane Models With 45° Sweptback Surfaces. NACA TN 2587, 1951.
19. Jaquet, Byron M., and Fletcher, H. S.: Lateral Oscillatory Characteristics of the Republic F-91 Airplane Calculated by Using Low-Speed Experimental Static and Rotary Derivatives. NACA RM L53G01, 1953.
20. DeYoung, John: Theoretical Additional Span Loading Characteristics of Wings With Arbitrary Sweep, Aspect Ratio, and Taper Ratio. NACA TN 1491, 1947.

TABLE I.- DIMENSIONS AND CHARACTERISTICS OF MODEL

Wing:

Airfoil section at fold (fold at $0.427 b/2$)	NACA 651-212
Airfoil section at theoretical tip	NACA 63-209
Total area, S_W , sq ft	2.04
Span, b_W , ft	3.47
Mean aerodynamic chord, \bar{c} , ft	0.613
Root chord (trailing edge extended), ft	0.762
Tip chord, ft	0.361
Sweep of leading edge, deg	0
Aspect ratio	5.90
Incidence, deg	
At theoretical root chord	-1/2
At theoretical tip chord	-1/2
At wing fold root chord	-1/2
Dihedral, deg	3

Horizontal tail:

Airfoil section	11-percent-thick NACA 65-series
Area, S_H , sq ft	0.485
Span, b_H , ft	1.51
Root chord, ft	0.402
Tip chord, ft	0.243
Sweep, leading edge, deg	8.45
Area ratio, S_H/S_W	0.238

Vertical tail:

Airfoil section	11-percent-thick NACA 65-series
Total area, S_V , sq ft	0.328
Root chord, ft	0.673
Tip chord, ft	0.268
Span, b_V , ft	0.694
Sweepback, leading edge, deg	24.50
Tail length, distance from center of gravity to $\frac{\bar{c}_V}{4}$, ft	1.42
Tail height, perpendicular distance from center of gravity	
to \bar{c}_V , ft	0.434
Area ratio, S_V/S_W	0.161
Fuselage length, ft	3.33

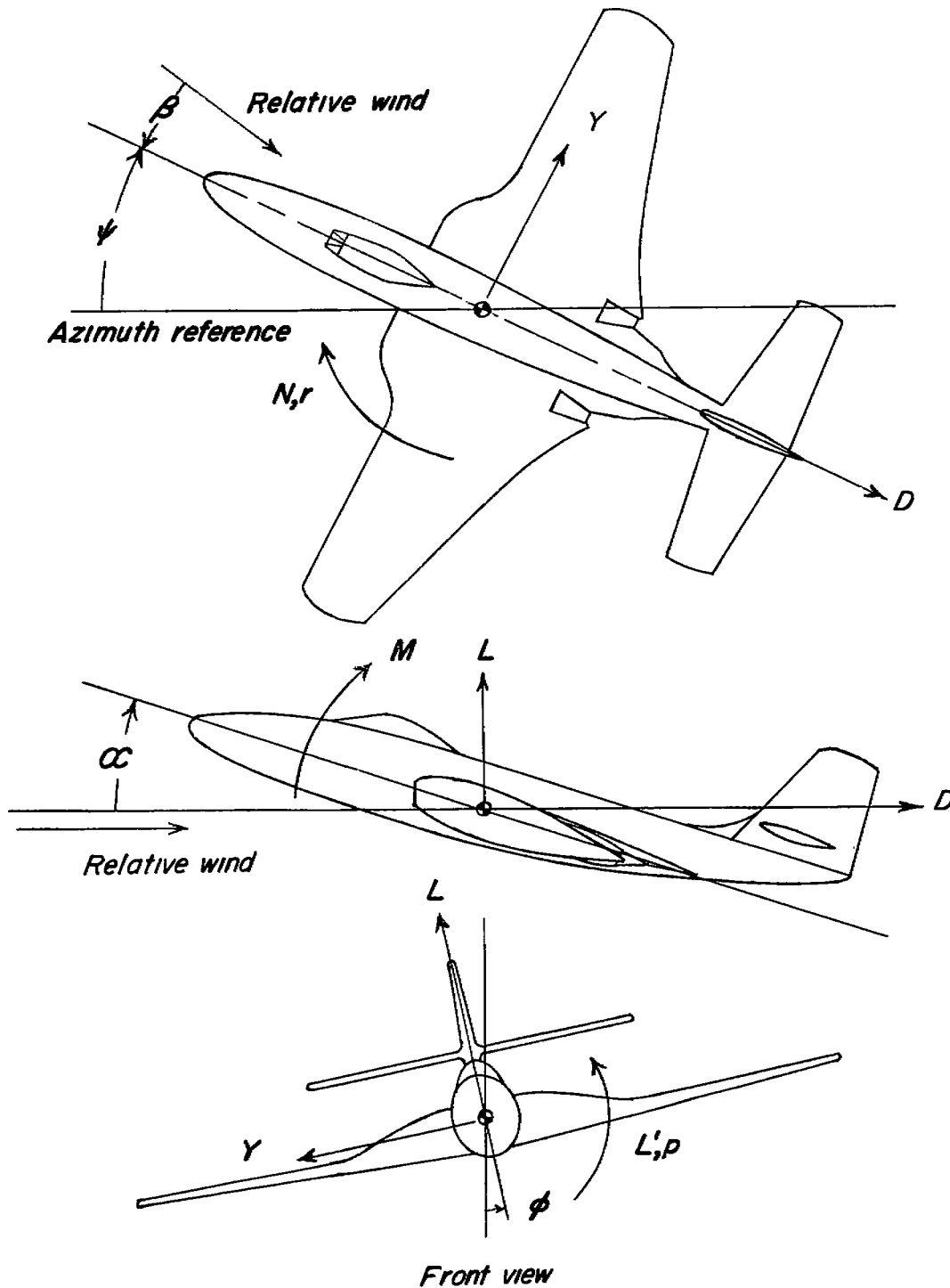


Figure 1.- System of stability axes. Arrows indicate positive direction of forces, moments, and displacements.

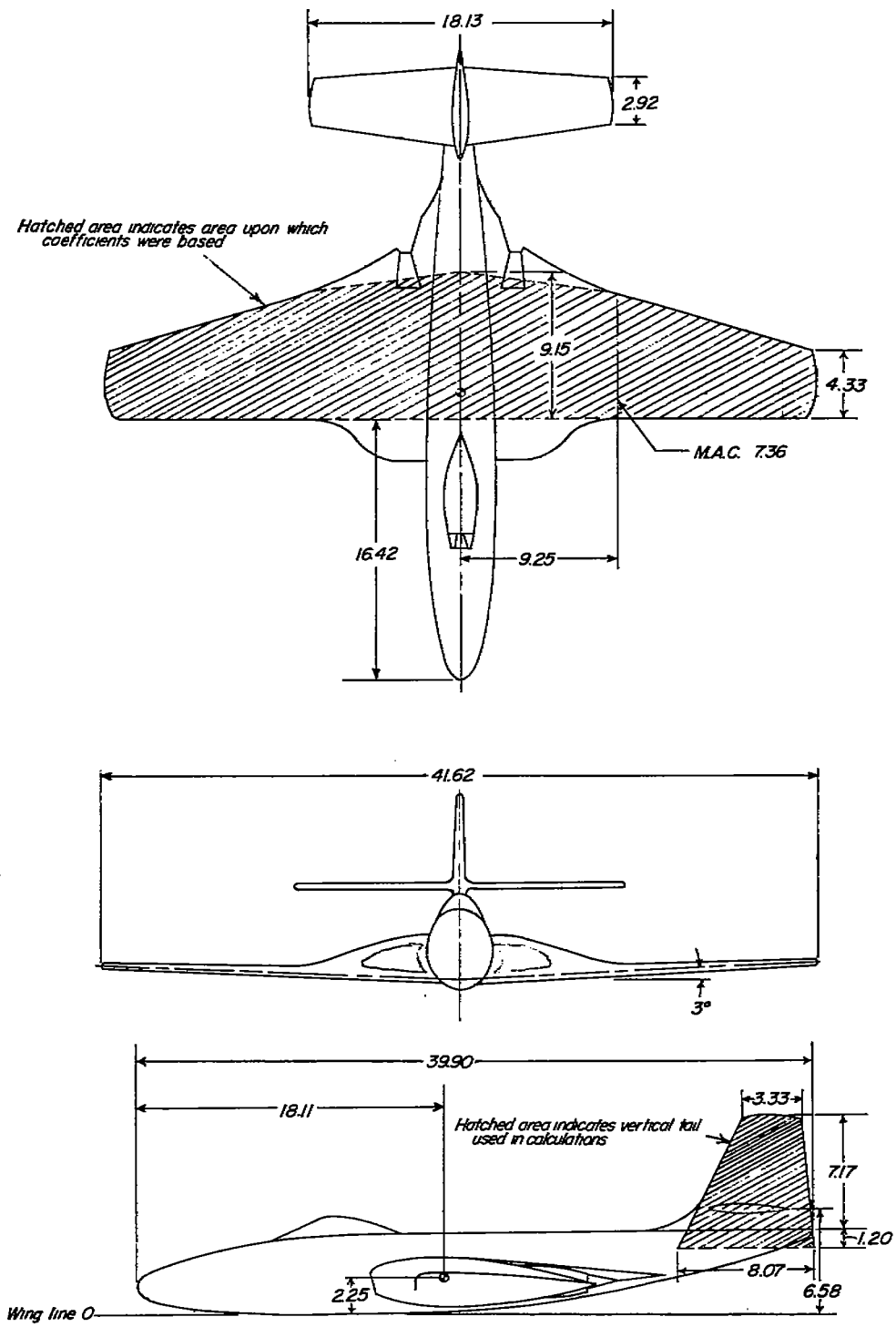
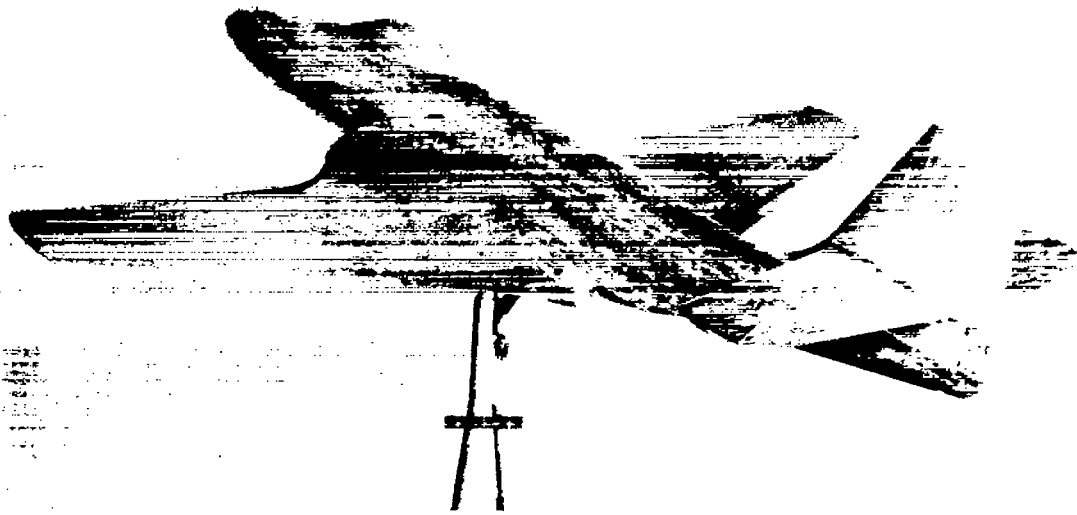


Figure 2.- Model used in the investigation. All dimensions are given in inches.



(a) View of complete model.

L-79633



(b) View of complete model with modified fuselage.

L-79634

Figure 3.- Model used in tests.

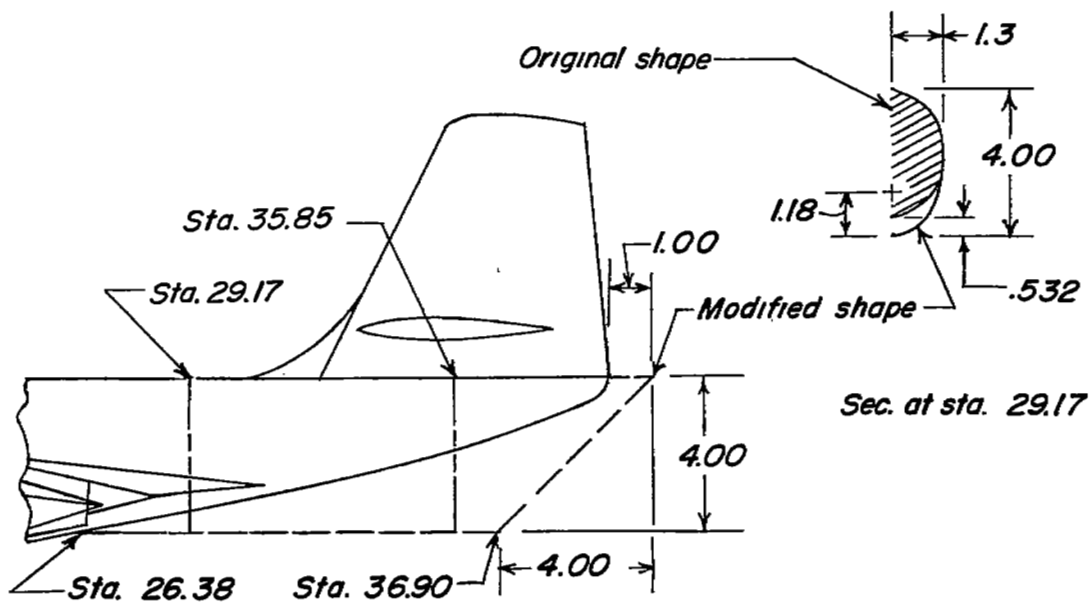
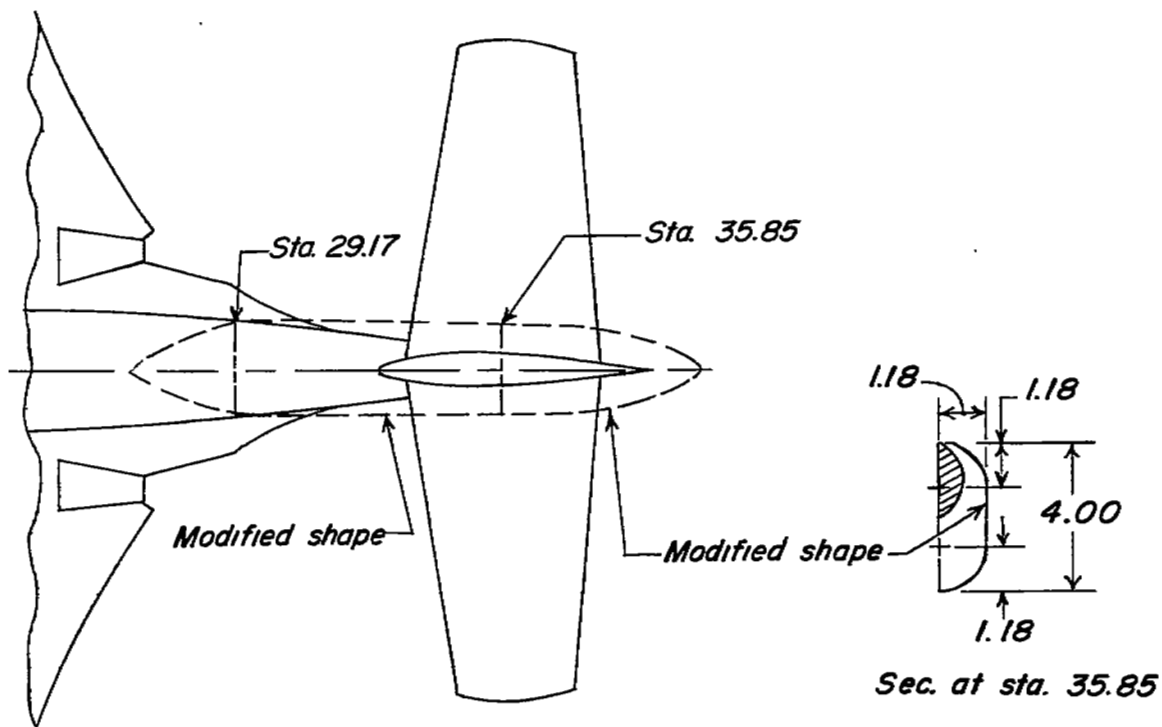


Figure 4.- Details of modified fuselage. All dimensions are given in inches.

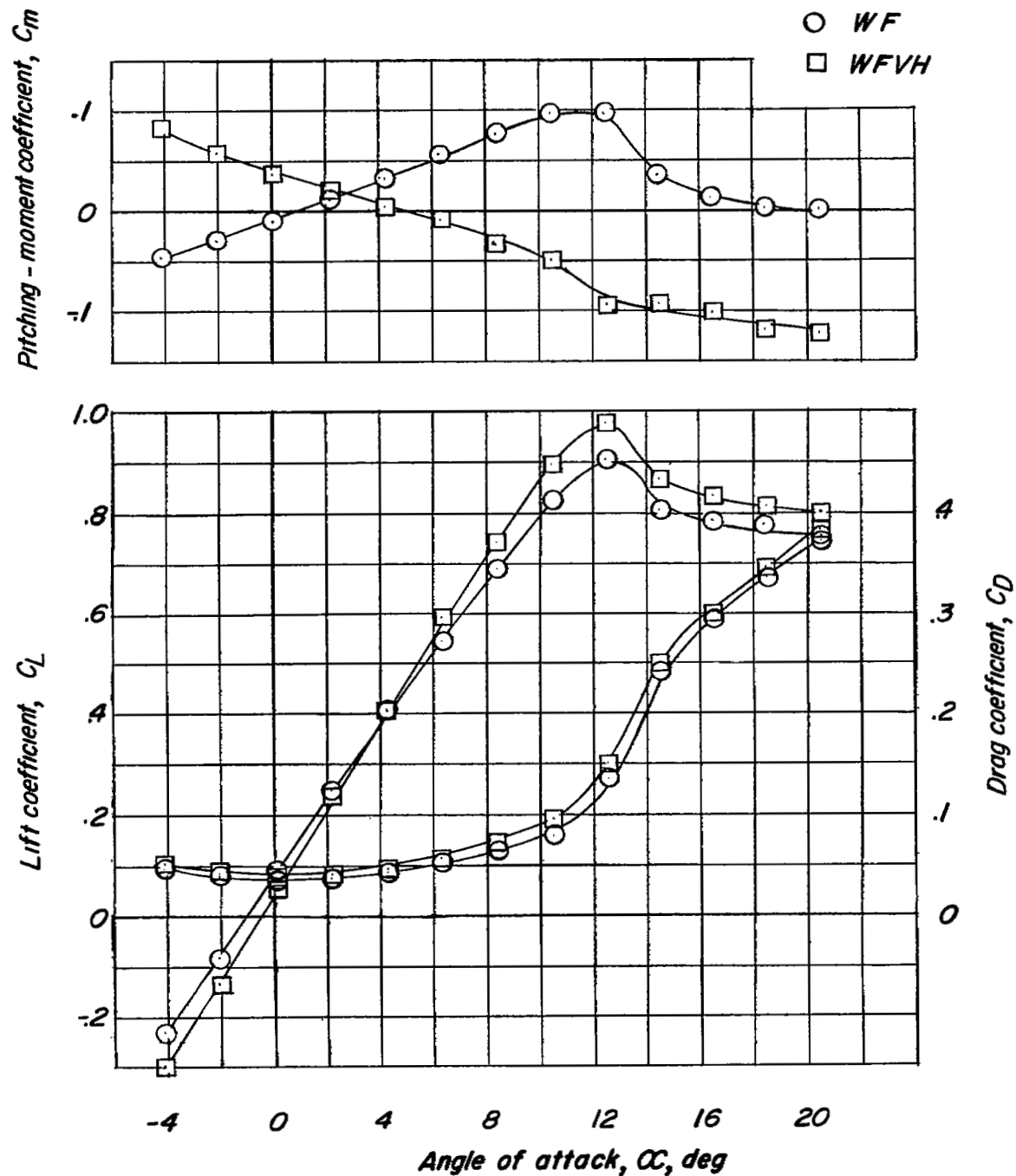


Figure 5.- Variation of lift coefficient, drag coefficient, and pitching-moment coefficient with angle of attack for wing-fuselage combination and complete model.

○ WF
 □ W F V H

Flagged symbols for modified fuselage - (see figs. 3 and 4)

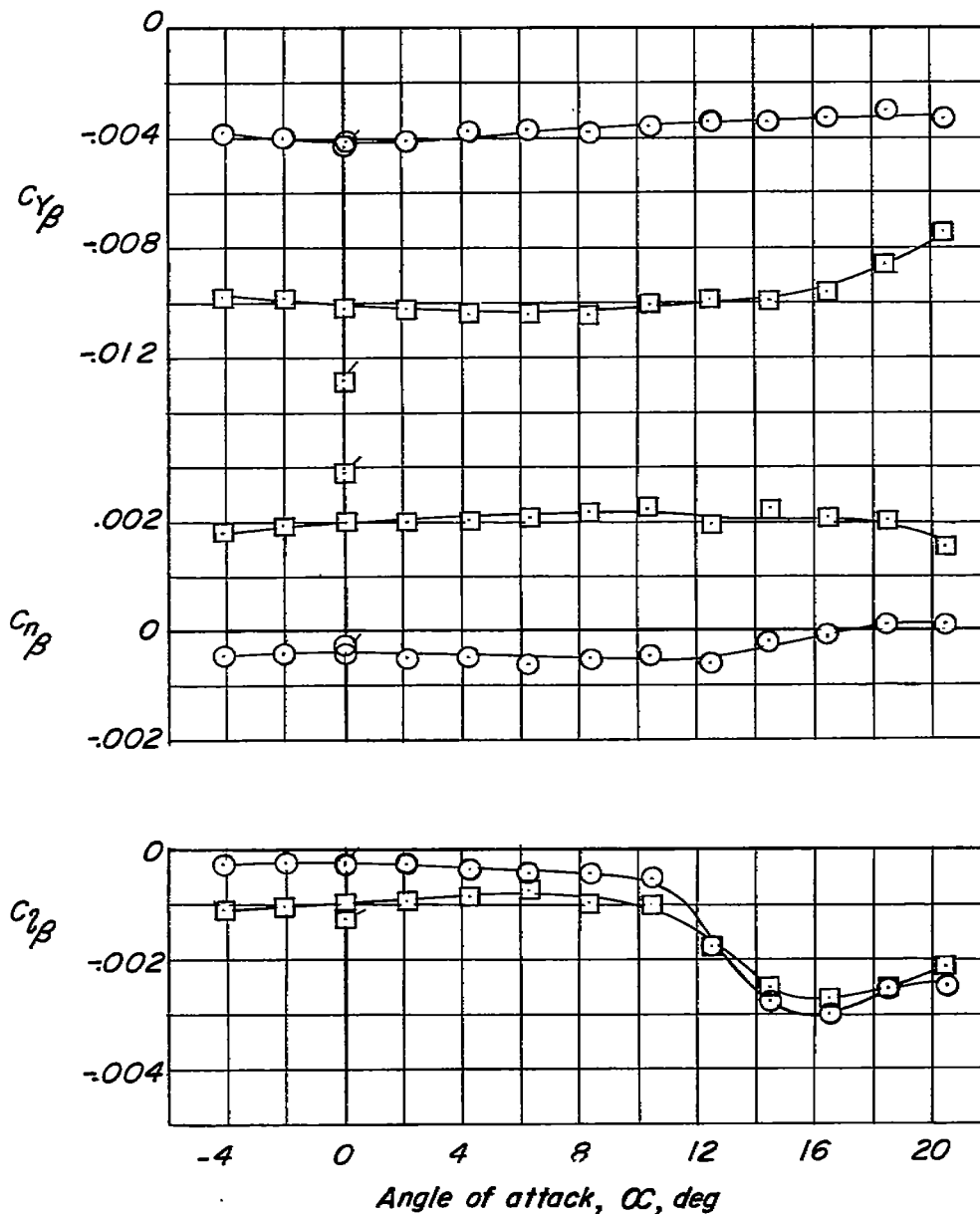


Figure 6.- Variation of static lateral stability derivatives with angle of attack for wing-fuselage combination and complete model. With and without rear fuselage modification.

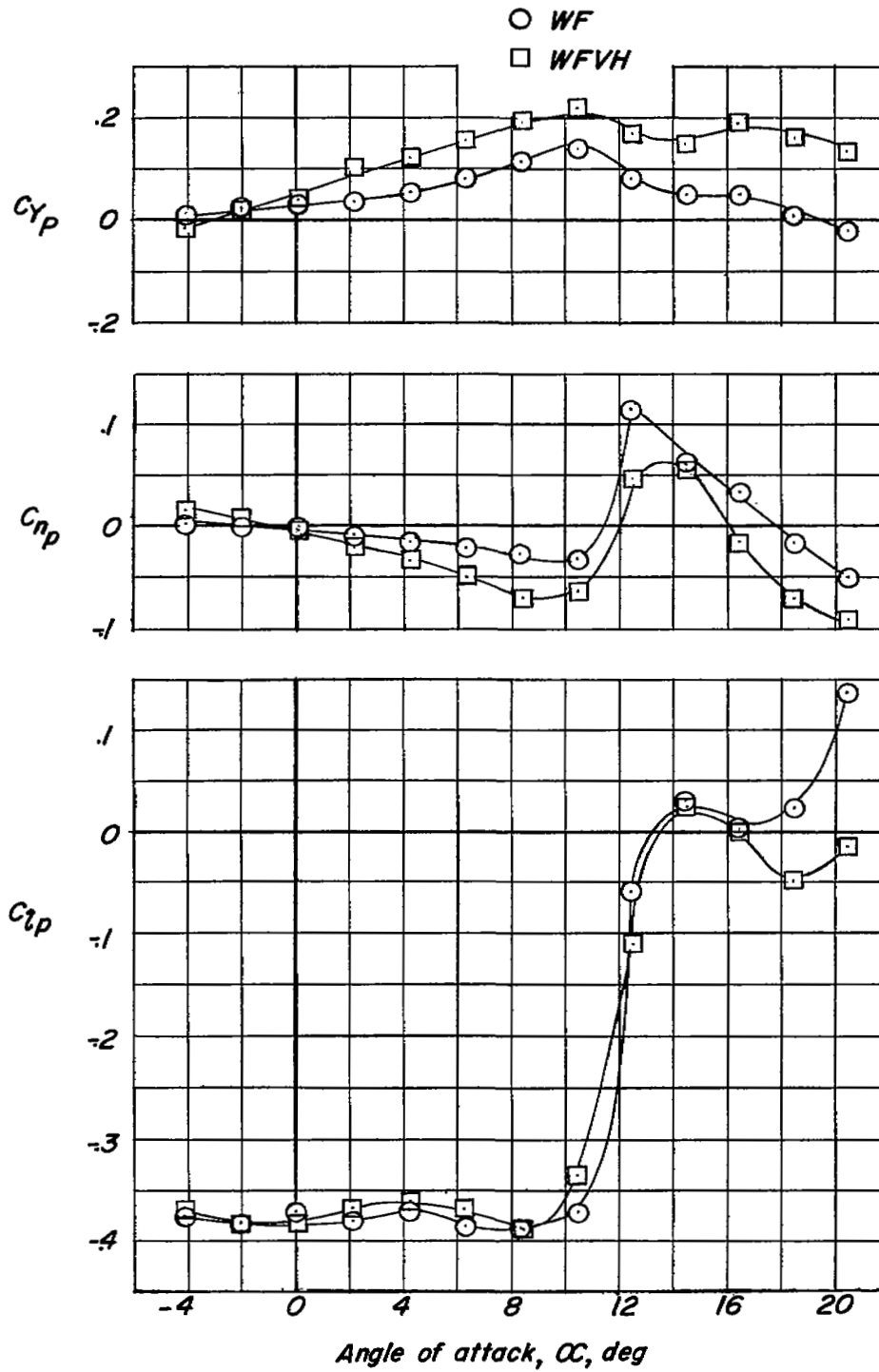


Figure 7.- Variation of rolling stability derivatives with angle of attack for wing-fuselage combination and complete model.

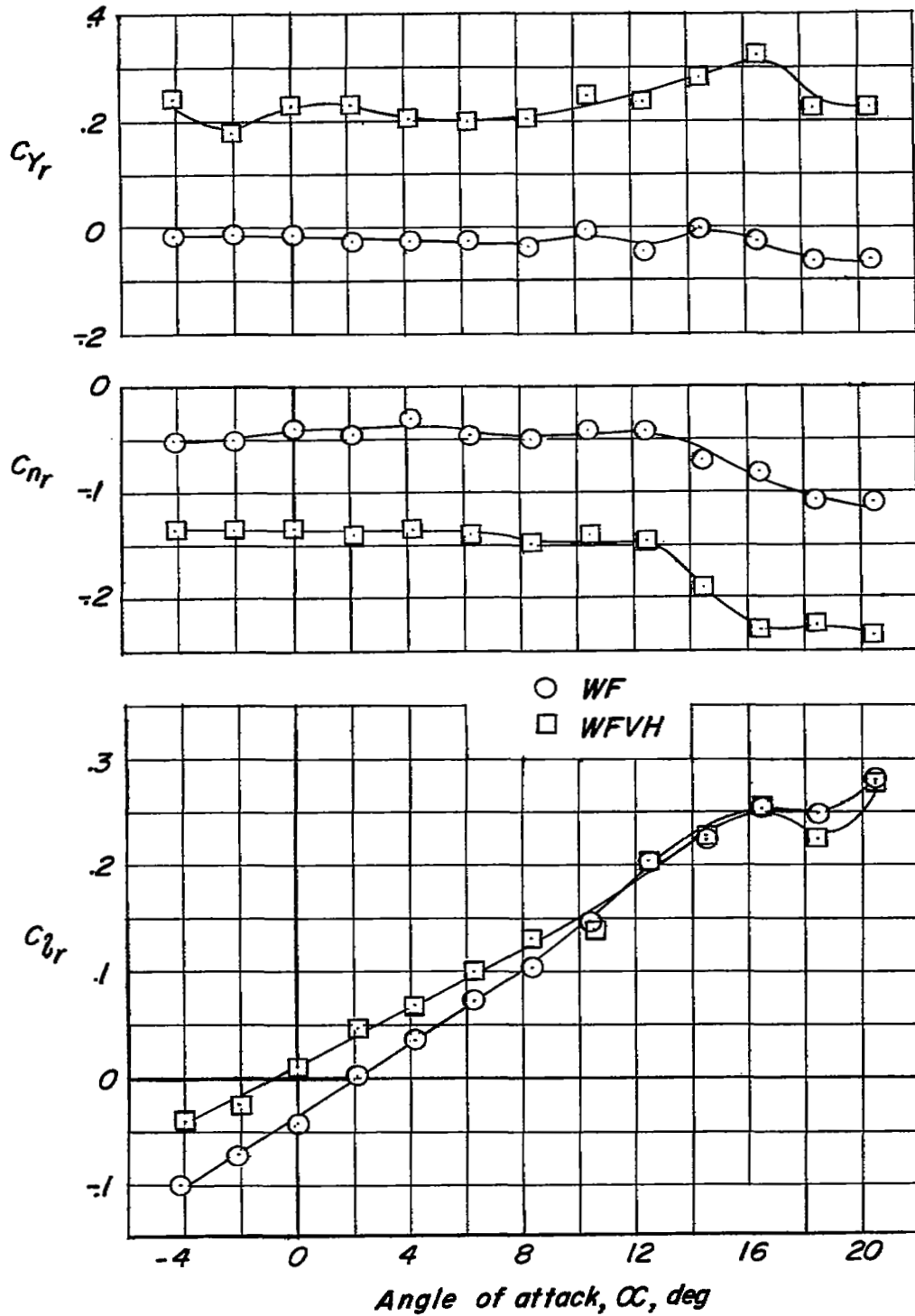
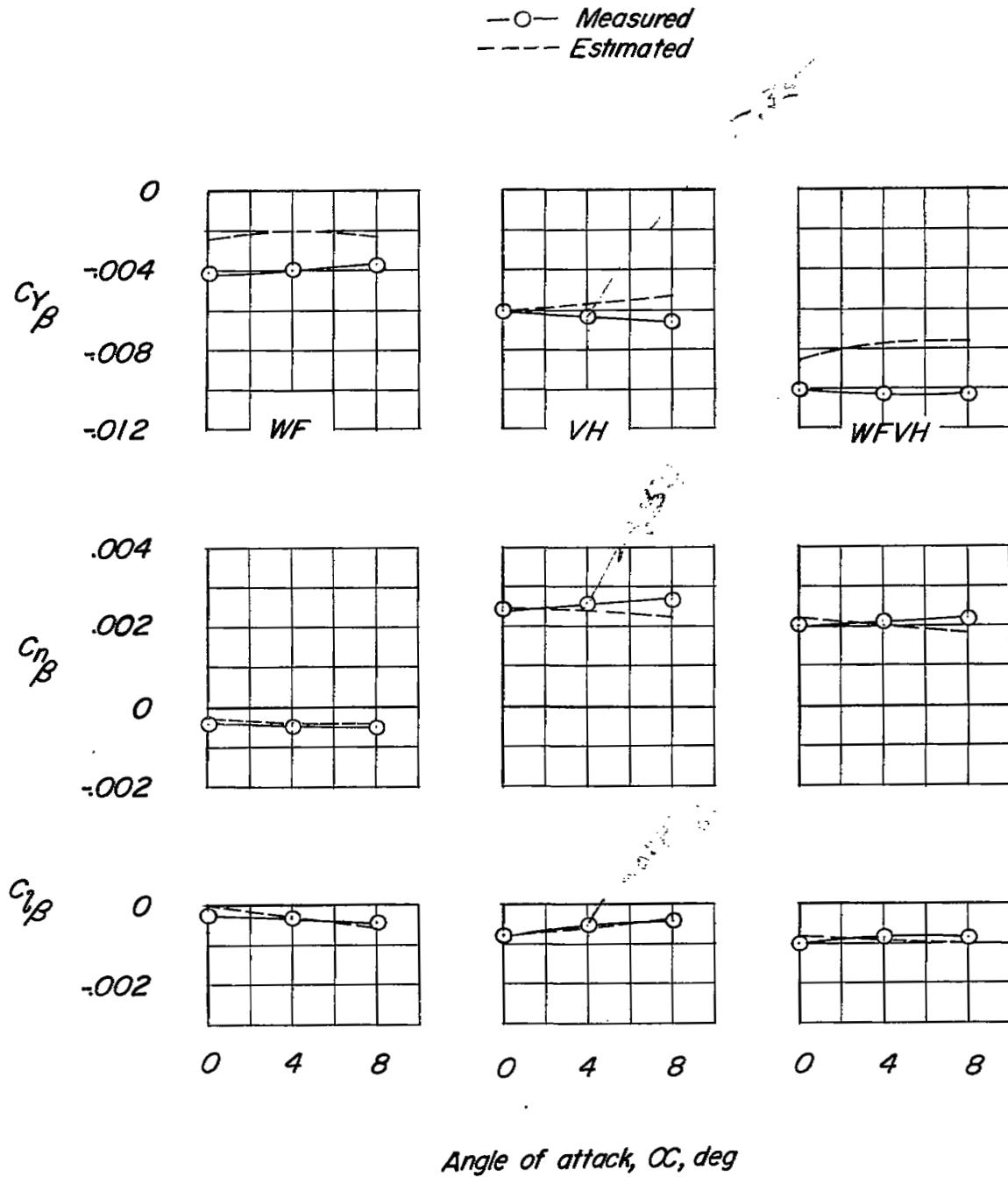
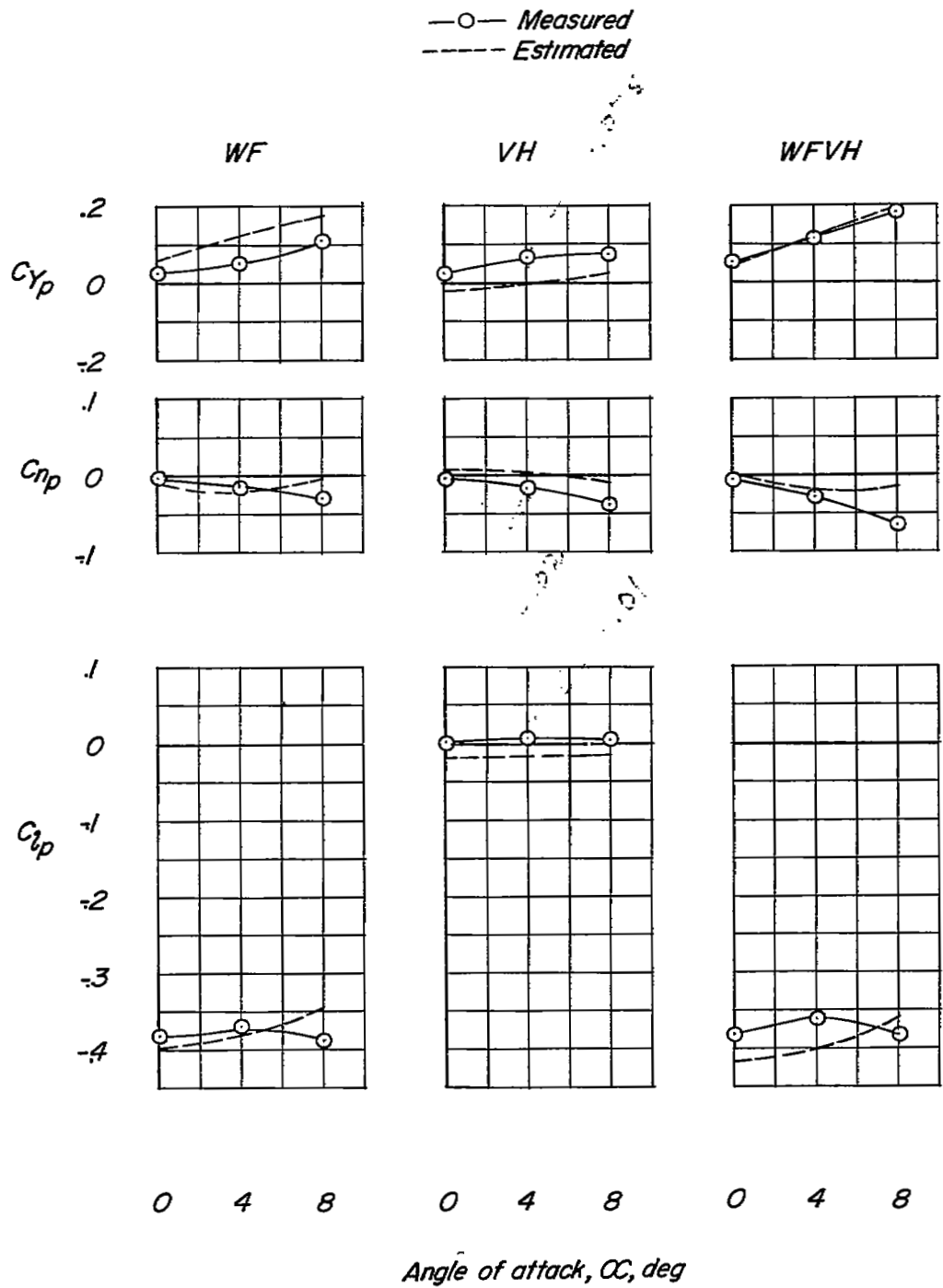


Figure 8.- Variation of yawing stability derivatives with angle of attack for wing-fuselage combination and complete model.



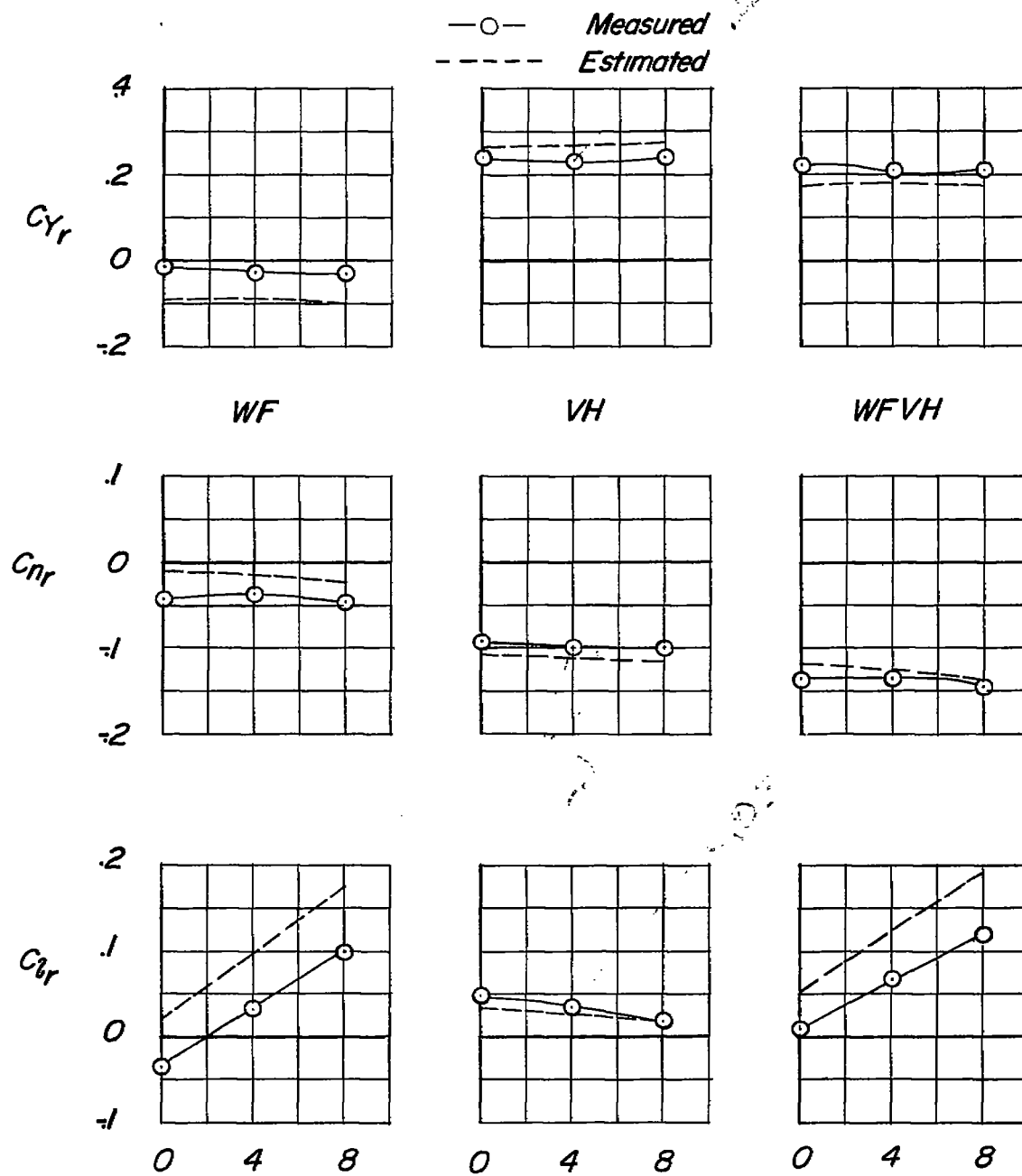
(a) Static derivatives.

Figure 9.- Comparison of the estimated and measured lateral and rotary derivatives for the wing-fuselage combination, vertical tail, and complete model.



(b) Rolling derivatives.

Figure 9.- Continued.



Angle of attack, α , deg

(c) Yawing derivatives.

Figure 9.- Concluded.